



OPEN

SUBJECT AREAS:

CELLULAR IMAGING

QUANTUM DOTS

NANOPARTICLES

MESENCHYMAL STEM CELLS

Mimicking cellular transport mechanism in stem cells through endosomal escape of new peptide-coated quantum dots

Karthikeyan Narayanan¹, Swee Kuan Yen², Qingqing Dou², Parasuraman Padmanabhan³, Thankiah Sudhaharan⁴, Sohail Ahmed⁴, Jackie Y. Ying¹ & Subramanian Tamil Selvan^{2,5}Received
15 April 2013Accepted
3 June 2013Published
15 July 2013

Correspondence and requests for materials should be addressed to K.N. (karthikeyan@ibn.a-star.edu.sg) or S.T.S. (subramanian@imre.a-star.edu.sg)

¹Institute of Bioengineering and Nanotechnology (IBN), A*STAR, 31 Biopolis Way, The Nanos, Singapore 138669, ²Institute of Materials Research and Engineering (IMRE), A*STAR, 3 Research Link, Singapore 117602, ³The Lee Kong Chian School of Medicine, Nanyang Technological University (NTU), Singapore 637553, ⁴Neural Stem Cell Group, Institute of Medical Biology, 61 Biopolis Drive, Singapore 138673, ⁵National University of Singapore, Division of Bioengineering, Faculty of Engineering, Singapore 117576.

Protein transport is an important phenomenon in biological systems. Proteins are transported via several mechanisms to reach their destined compartment of cell for its complete function. One such mechanism is the microtubule mediated protein transport. Up to now, there are no reports on synthetic systems mimicking the biological protein transport mechanism. Here we report a highly efficient method of mimicking the microtubule mediated protein transport using newly designed biotinylated peptides encompassing a microtubule-associated sequence (MTAS) and a nuclear localization signaling (NLS) sequence, and their final conjugation with streptavidin-coated CdSe/ZnS quantum dots (QDs). Our results demonstrate that these novel bio-conjugated QDs enhance the endosomal escape and promote targeted delivery into the nucleus of human mesenchymal stem cells via microtubules. Mimicking the cellular transport mechanism in stem cells is highly desirable for diagnostics, targeting and therapeutic applications, opening up new avenues in the area of drug delivery.

In the mammalian cell, the cell membrane acts as a barrier to cargoes (ions, small molecules or macromolecules). In higher order biological systems, a nuclear localization signal (NLS) is essential for targeting macromolecular cargoes to the nucleus. Studies on stem cells hold much promise for human regenerative medicine. Recent advances in the field of nanoparticles (NPs) generated novel applications in biomedicine including regenerative medicine. Applications such as imaging, diagnostics and drug delivery (the so-called theranostics) require precise targeting approach for their successes^{1–4}. NPs have been engineered to induce membrane receptor internalization, followed by downstream signaling and subsequent cellular responses. NP-mediated cellular response is size-dependent⁵. Gold NPs have been shown to be a powerful vehicle for drug delivery⁶. The presence of Herceptin–gold NP complexes within endosomes showed that receptor-mediated uptake is the most probable mechanism. There are several biological barriers at the cellular level that the engineered NPs must overcome, starting from cell membrane to sub-cellular compartment (cytosol, mitochondria or nucleus). Several endocytic mechanisms can be engaged to facilitate the internalization of a carrier. In clathrin-mediated endocytosis, endosomal escape must occur before fusion with a lysosome to prevent degradation of the cargo by the harsh lysosomal conditions. More importantly, the endosomal escape is usually necessary to allow access of the carrier to the desired sub-cellular compartment⁷. For example, the uptake of TAT-functionalized Au NPs was enhanced in HeLa cells and the particles initially found in the cytosol, nucleus, mitochondria and later within densely filled vesicles were released, negotiating intracellular membrane barriers quite freely, including the possibility of direct membrane transfer⁸.

The intracellular delivery of quantum dots (QDs) is mainly governed by size, surface charge and coatings^{9–11}. Different types of peptides have been used as the promising candidates for intracellular delivery of QDs^{9–15}. Recent advances include the enhancement of intracellular delivery of streptavidin-conjugated QDs into mouse fibroblast cells using biotinylated L-arginine peptides¹⁰, TAT-functionalized QDs for selective intracellular transport, vesicle shedding and delivery^{9,13,14}. Arginine–glycine–aspartic acid (RGD) peptides have been conjugated to target QDs specifically to tumor angiogenesis for theranostics^{12,16}. Despite these advances, the effective nuclear targeting (since many of the anti-cancer targets are located in the nucleus) and therapeutic applications of QDs are still



limited by their poor intracellular delivery and aggregation within the endosomes. We have chosen CdSe QDs as a model system owing to their superior optical properties and stability. Here we show a simple approach for the effective nuclear targeting via microtubules using a combined peptide approach involving both NLS and microtubule-associated sequence (MTAS) peptide-QD conjugates.

Results

Importance of endosomal escape and designing of peptide sequences. In the area of NP-mediated drug delivery, it is assumed that only <10% of active drugs would escape the endosomes and reach the nucleus. Therefore, an endosomal escape is highly indispensable. To achieve this, we have initially designed a peptide sequence based on NLS and a transport protein (TP); the latter has been used for the delivery of siRNA/proteins/PNA^{17–19}. First, we demonstrate the design of a novel peptide sequence containing TP and SV40-NLS peptides to elucidate the nuclear targeting via endosomal escape using CdSe/ZnS QD-peptide conjugates. In another interesting design, we could mimic the cellular protein transport pathway using MTAS and NLS peptide-QD conjugates. We believe this combined strategy would increase the endosomal escape of cargoes, and be useful for optimal drug delivery to the nucleus. We have systematically designed and studied different peptides (SV40-NLS, TP, short MTAS (s-MTAS) and long MTAS (l-MTAS)) to determine which one of them is more efficient in delivering the QDs to cell organelles, e.g. the nucleus for effective targeting (Fig. 1). We will show the efficacy of peptide coating

method for labeling stem cells and transporting QDs to the nucleus via microtubules using mixed NLS and l-MTAS peptides. We believe that this is the first report of nuclear targeting of QDs through microtubules using a biomimetic approach.

QD-peptide conjugates. Our initial study suggested that a short chain peptide, e.g. glutathione (GSH) can be used in transferring the CdSe/ZnS QDs into water. The peptide coating of QDs was performed in Igepal reverse micelles (see Methods). The peptide-coated QDs were purified by several rounds of centrifugation in ethanol before they were dispersed in water or buffer solutions. We have also analyzed the effects of peptide coating method on plain CdSe QDs (i.e. without ZnS shell). The emission of CdSe QDs coated with NLS peptides at 520 nm was more intense and sharp as compared to the QDs coated with NLS and TP peptides (Supplementary Fig. S1). In literature, the trioctyl phosphine oxide (TOPO) ligands on the QDs are often exchanged with thiol-functionalized compounds such as mercaptoacetic acid²⁰, dihydrolipoic acid²¹, dithiothreitol²² and cysteine-containing peptides²³. The QDs have also been coated with inorganic silica^{24–27} or organic protective polymer²⁸. Silica and polymer coatings significantly increased the overall size to >20 nm, and restricted their use to certain imaging applications. In contrast, our peptide-coated QDs exhibited a mean particle diameter of only 6 nm.

Conventional nuclear targeting with SV40-NLS. The transport of CdSe/ZnS QDs coated with SV40-NLS and SV40-NLS-TP peptides

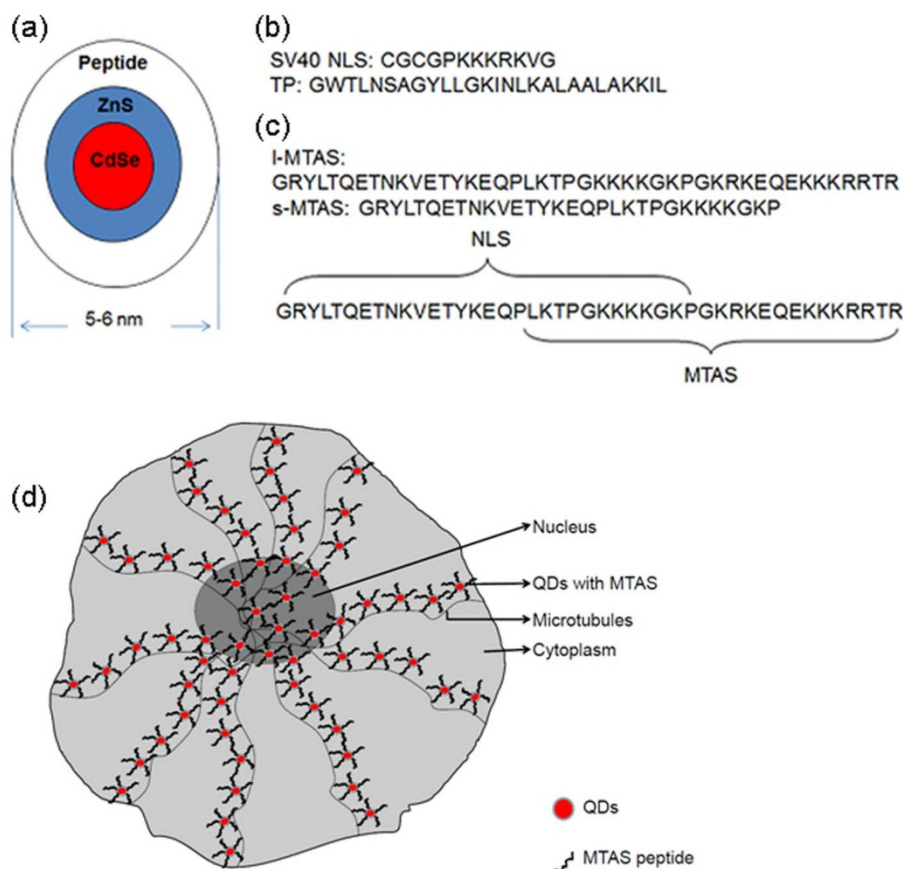


Figure 1 | Design of different peptide sequences for making water-soluble core/shell CdSe/ZnS quantum dots (QDs). (a) A cartoon showing the mean diameter of peptide-coated QDs. (b) Peptides used in this study: SV40 NLS – nuclear localization signalling sequence, TP – transport protein. (c) Peptide sequence deduced from parathyroid hormone related protein (PTHrP). The microtubule associated sequence (MTAS) domain spans 17–44 amino acids, while NLS spans 1–30 amino acids. Long (l-) MTAS represents 1–44 amino acids while short (s-) MTAS represents 1–30 amino acids. The s-MTAS lacks the complete sequence required for the association with microtubules. (d) A schematic illustration of the transportation of QDs to the nucleus of hMSCs via microtubules.



is illustrated in Fig. 2. While significant nuclear labeling (presumably due to endosomal escape) is observed with NLS-TP-coated QDs (Figs 2a and 2b), the nuclear labeling efficiency appeared to be low with NLS-coated QDs (Figs 2c and 2d). Conversely, the control GSH-coated QDs were found to be accumulated in the endosomes of human mesenchymal stem cells (hMSC) (Supplementary Fig. S2). Our observations are in consonance with earlier studies in the literature that showed the co-localization of similar CdSe/ZnS QDs coated with polyethylene glycol (PEG) grafted polyethylenimine (PEI-g-PEG), which penetrated the cell membrane and were trapped in endosomes²⁹. In a very recent report, the association of QDs in early endosomes and late endosomes was colocalized by EEA1 and CD63 antibodies, respectively³⁰. These co-localization studies and our control GSH labeling further corroborated the endosomal escape of NLS-TP peptide-coated QDs.

Microtubule associated QD transport for efficient nuclear targeting. Cytoskeleton, the cellular scaffold, is composed mainly of microtubule and actin filaments. The microtubule is composed of tubulin filaments, which helps in various cellular activities such as signaling, macromolecular cargo and nucleic acid transport between the nucleus and other compartments of the cell³¹. The nuclear compartment of a cell is separated from the rest of the cell by a nuclear envelope, which contains nuclear pore complex for the transport of macromolecules that are anchored with NLS sequence. The transport of proteins on the microtubule elements is called axonal transport, which is well studied in neuronal cells. This transport is facilitated by complex motor proteins involving various kinesin molecules³². Importantly, many proteins such as cancer related protein p53^{33,34} and parathyroid hormone related protein (PTHrP)³⁵ are dependent on the microtubules for efficient nuclear transport. PTHrP harbors a specific sequence that can interact with microtubules for its facilitated transport and the peptide sequence responsible for this interaction is called microtubule associated sequence (MTAS).

To mimic the microtubule assisted cargo transport, we have designed peptides that were reported in the biological systems (PTHrP) to bind microtubules. The sequence identified in PTHrP (containing NLS and MTAS domains) spans ~44 amino acids

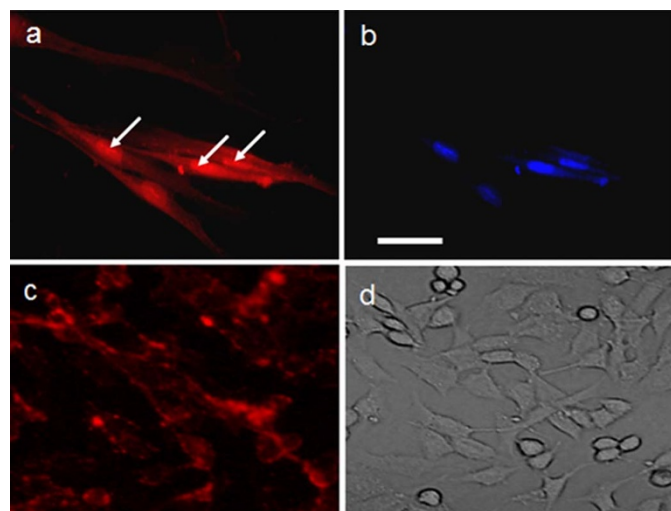


Figure 2 | Labeling of hMSCs. (a,b) SV40-NLS-TP and (c,d) SV40-NLS peptide-coated red-emitting CdSe/ZnS QDs. See Figure 1 for the anatomy of peptides. (a, c) Cells under fluorescence microscope. (b) DAPI staining indicating the nucleus of the cell. White arrows in (a) point out the accumulation of QDs in the nucleus. (d) Light microscope image. It is clear from (c) that SV40-NLS peptide-coated QDs are present on the cell membrane and endosomes without nuclear targeting. Scale bar: 100 μm .

(Fig. 1). However, the MTAS domain resides at the c-terminal region of the peptide sequence and spans 27 amino acids, while the NLS domain spans 30 amino acids upstream of MTAS domain. l-MTAS consists of both NLS and MTAS domains, while s-MTAS contains only the NLS with partial MTAS domain. We tested the feasibility of l-MTAS and s-MTAS for their ability to transport the QDs via microtubules. To test the targeting concept, we have also used biotinylated peptides and red/green streptavidin-QDs. The transport of QDs via microtubules prior to reaching the nucleus in hMSCs using l-MTAS is clearly observed (Figs. 3a and 3b). The detailed images of different channels are shown in the Supplementary Fig. S3. We also imaged different locations of a single cell at higher magnification and ‘stitched’ the images to generate a complete image (Supplementary Fig. S4). These images convinced us that the QDs were transported via microtubules to the nucleus. s-MTAS conjugated QDs did not show the transport along the microtubules. Most of the QDs were trapped on the membrane of the hMSCs (Fig. 3c). This illustrated that the presence of NLS sequence alone was not sufficient to target the QDs to the cell nucleus. More distinctly, we did not observe the microtubule assisted transport of the s-MTAS-QDs, which showed that the l-MTAS domain was necessary for the active transport of QDs via microtubules. Our results were similar to the observations made on the biological systems. Earlier studies with deletion of the MTAS domain resulted in the random accumulation of mutant outside the cell nucleus³⁶.

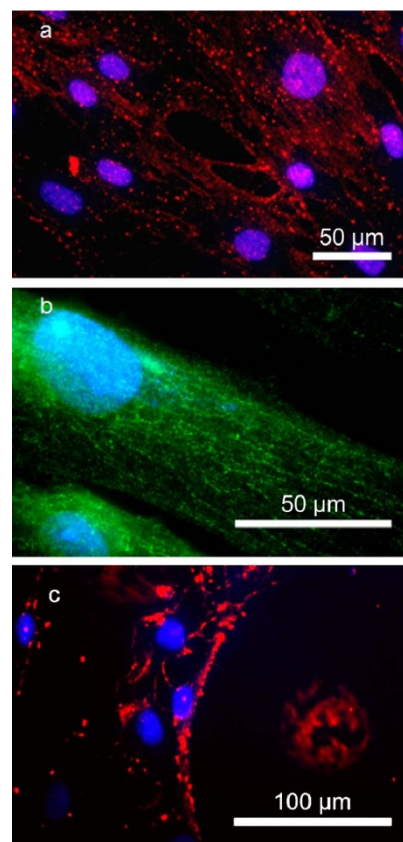


Figure 3 | Microtubule assisted transport of QDs. Nuclear transport of streptavidin-QDs conjugated with biotinylated l-MTAS of (a) red emission and (b) green emission in hMSCs. The nuclear compartment is stained with DAPI (blue). The transport via microtubules and nuclear accumulation of QDs can be clearly seen. (c) Transport of QDs (red) conjugated with s-MTAS peptide. The s-MTAS peptide lacks the complete MTAS domain and thus is not able to transport QDs via microtubules. The cell nucleus is stained with DAPI (blue).



Co-localization of l-MTAS-QD with anti-tubulin antibody. In order to further confirm the transport of the QDs via microtubules, we performed co-localization staining experiments with anti-tubulin antibodies. In Fig. 4, microtubule is stained with anti-tubulin–Alexa Fluor-488 secondary antibody, the nucleus is stained with DAPI, and the red channel is stained with streptavidin-coated CdSe/ZnS QDs conjugated with biotinylated l-MTAS. Anti-tubulin antibody staining confirms the arrangement of microtubules (Fig. 4a). It is clear that the QDs are organized in a fashion similar to the microtubule distribution and there is a clear accumulation of QDs in the nucleus (Fig. 4b). DAPI is used to stain the nuclear compartment (Fig. 4c). Overlaying the red, green and blue channels distinctly illustrates the alignment of QDs on the microtubules of hMSC and the accumulation of QDs in the nucleus (Fig. 4d). The presence of l-MTAS-QDs on the tubulin filaments was further confirmed by the zoomed images taken on a part of hMSC under high magnification (Supplementary Fig. S5). On the other hand, staining the actin filaments with phalloidin–Alexa Fluor 488 showed that the QDs were not co-localizing with actin filaments, suggesting the microtubule specific association of MTAS peptide (Supplementary Fig. S6). Additionally, confocal laser scanning microscopy was used to further confirm the co-localization of l-MTAS-QDs with tubulin filaments. Z-stack scanning was done on the samples stained with anti-tubulin antibody. Orthogonal analysis of the z-stacks confirms the presence of l-MTAS-QDs on the tubulin filaments (Fig. 5a). Next, we quantitatively estimated the fluorescence intensity in the nuclear compartment of the cells incubated with QDs containing SV40-NLS, SV40-NLS-TP, l-MTAS and s-MTAS using Image J software (freeware from NIH). We measured the intensities of entire cell (total) and nuclear compartments of several individual cells in each group. The ratio of fluorescence intensity between nuclear and total cell labeling is much higher for l-MTAS conjugated QDs (Fig. 5b).

Requirement of microtubules for nuclear transport. To further confirm the microtubules assisted delivery of QDs to the nucleus, we disrupted the microtubule assembly with a small molecule, nocodazole, which is commonly used in biological experiments to validate the functional role of microtubules. We found that the uptake of QDs was very low or almost none in the nocodazole-treated hMSCs

(Fig. 6a). The DAPI stained nucleus is shown in Fig. 6b. Anti-tubulin antibody staining of hMSCs treated with 5 $\mu\text{g}/\text{ml}$ of nocodazole clearly indicated the disrupted cytoskeletal elements (Figs 6c and 6d). These results further confirmed that QDs with MTAS peptides required microtubules for their efficient internalization and transport to the nucleus.

Discussion

In this communication, we have presented a novel method to transport the QDs to the nucleus of hMSC through microtubules. The successful delivery of NPs, drug molecules or genes into sub-cellular compartments requires a clear understanding of the cellular machinery in order to keep the cell functions intact. Advances in molecular and cellular technologies have identified many anti-cancer targets including signal transducer and activator of transcription (STAT) proteins and Karyopherin beta proteins in the nucleus³⁷. The most commonly used methods for the delivery of genes into the nucleus of cells are viral and non-viral vectors. Often, this method raises the safety concerns for precise delivery of gene products.

Earlier, cell penetrating peptides (CPP) were used to cross the cell membrane for cytosolic delivery. It is worth mentioning here that the structurally ordered ligand shell morphology³⁸ of striped Au NPs (analogous to CPP) penetrated the membrane and internalized into cytosol of the cell, whereas similar particles but with unordered ligands on the surface resulted in trapping within endosomes³⁹. Interestingly, passive (e.g. CPP, proton sponge polymer carrier) and active targeting methods (e.g. electroporation, microinjection) have been developed to deliver QDs into the sub-cellular targets. Recently, a photothermal nanoblade method was used to deliver the tubulin-coated QDs onto growing microtubules in the cytoplasm of HeLa cells⁴⁰.

Although the use of protein sequences to transport genes into specified location of cells especially to the nucleus through microtubules has been successful, the sequence specificity is debatable. Here, we have combined the peptide sequence of both NLS sequence and microtubule binding sequence of PTHrP³⁵ protein for targeting QDs into the nucleus. Our data suggest that NLS sequence alone will not be sufficient to transport QD to the nucleus, but combining the l-MTAS sequence with NLS makes it a more distinct method for efficient transport to the nucleus. In addition, our studies on the

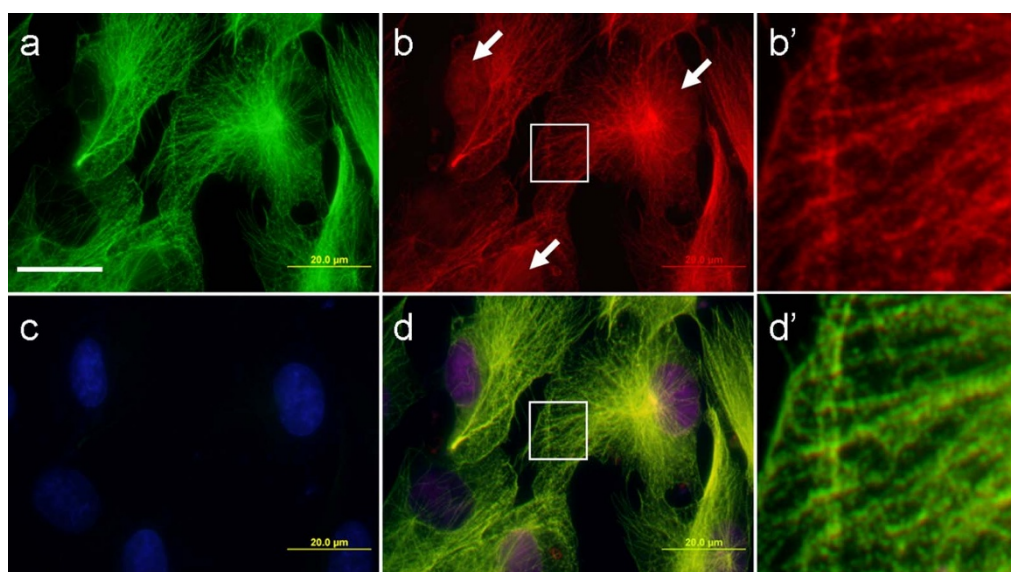


Figure 4 | Co-localization of l-MTAS QDs, anti-tubulin antibody and DAPI in hMSC. (a) Anti-tubulin antibody (green), (b) QDs conjugated to l-MTAS (red), (c) DAPI (blue) and (d) Composite image. The alignment of QDs on the microtubules and nucleus labelling (d) are clearly seen. The white arrows mark the presence of QDs in the nucleus (b). The regions corresponding to the white boxes in (b) and (d) were enlarged and shown in (b') and (d') respectively. Scale bar = 20 μm .

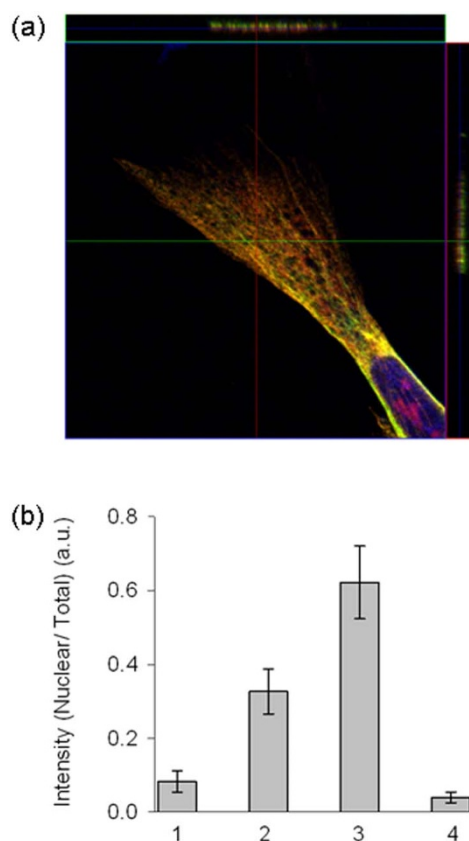


Figure 5 | Z-stack imaging for the co-localization of I-MTAS-QDs on the tubulin filaments observed by confocal laser scanning microscope. (a) Z-stack imaging and orthogonal analysis of the stained cells. Scanning was done along the lines drawn on adjacent extensions of the image. (b) The efficiency of nuclear targeting for the four different peptides reported here. The total cellular fluorescence and nuclear compartment fluorescence were measured for five cells of each group. The efficiency of the nuclear targeting was measured as the ratio of fluorescence intensity between nucleus and total hMSC labeling (represented as nuclear/total). X-axis represents the different peptide groups: 1, 2, 3 and 4 corresponding to SV40-NLS, SV40-NLS-TP, I-MTAS and s-MTAS, respectively.

non-co-localization of QDs with phalloidin and microtubule disruptions using nocodazole confirm the specificity of this sequence required for the transport through microtubules. The complete co-localization of QDs with microtubules while transporting to the nucleus confirms the sequence accuracy of our method.

In summary, we have demonstrated for the first time a biomimetic transport of QDs to the nucleus of the adult stem cells. We have demonstrated two new methods for the nuclear targeting of QDs. The first one was based on the combination of two long chain peptides (NLS and TP), which enabled the release of CdSe/ZnS QDs from endosomes. The second approach mimicked the cellular protein transport pathway via microtubules. Co-localization and tubulin disruption studies have highlighted clearly the mode of transport of QDs to the nucleus. We have also found that the QDs could be delivered more efficiently into the nuclei of the cells. The higher nucleus labeling efficiency of over 60% confirmed the advantage of the microtubule-associated delivery in comparison with other methods. We believe this precise targeting approach can be extended to anti-cancer targets within the nucleus, and hence open up new avenues in drug delivery applications.

Methods

General. All chemicals required for QD synthesis were purchased from Sigma-Aldrich, and used as received without further purification. SV40-NLS, TP and

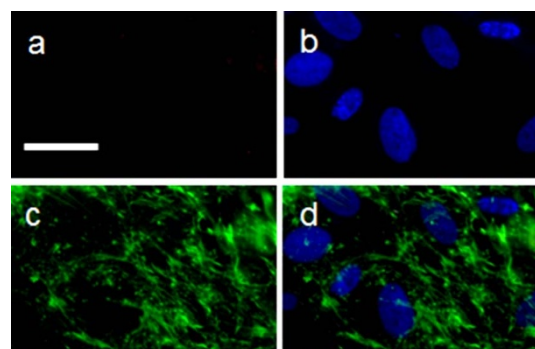


Figure 6 | Microtubule disruption results in no uptake of QDs. hMSCs were treated with 5 $\mu\text{g}/\text{ml}$ of nocodazole for 4 h prior to the addition of I-MTAS-conjugated QDs. The cells were fixed and stained with QDs (a) and DAPI (blue, (b)). The disrupted microtubules can be seen with anti-tubulin antibody staining (green, (c)) and in the composite image (d). It is clear that the uptake of QDs conjugated with I-MTAS peptide is inhibited completely in the absence of organized microtubules (a). Scale bar: 50 μm .

biotinylated MTAS-NLS peptides were obtained from GL Biochem Ltd (Shanghai, China). Emission spectra were acquired with a Fluorolog FL 3-11 fluorometer using a quartz cell with 1-cm path width.

Synthesis of CdSe/ZnS QDs. All syntheses were performed in air-free atmosphere in a blanket of Ar. Highly luminescent CdSe/ZnS QDs (quantum yield = 60%) were synthesized using stearic acid (SA), TOPO and tetradecylphosphonic acid (TDPA) in accordance with literature procedures^{41,42}. In a typical synthesis, CdO (0.05 g, 0.39 mmol) and SA (1.3 g, 4.57 mmol) were loaded into a three-necked flask and pumped under vacuum for 20 min. The mixture was heated under Ar to $\sim 200^\circ\text{C}$ to form cadmium stearate, resulting in a clear solution. After being cooled to room temperature, the flask was further charged with TDPA (0.16 g, 0.57 mmol) and TOPO (7 g, 18.1 mmol), and heated to 280°C . Se (0.32 g, 4 mmol) dissolved in trioctylphosphine (TOP) (8 g, 21.6 mmol) was injected swiftly and held at that temperature for a different growth period to reach the desired size for green and red emitting QDs. The reaction was then cooled to 190°C , and a mixture of 6 mL of diethyl zinc ($\text{Zn}(\text{Et})_2$, 1.1 M in toluene) dissolved in 8 mL of TOP and 1.5 mL of hexamethyl disilathiane was gradually injected over 10 min. The reaction was allowed to proceed for 1 h at 180°C . Finally, the heating mantle was removed, and the reaction was cooled to $40\text{--}50^\circ\text{C}$; 10 mL of chloroform was added to avoid the solidification of TOPO. Excess capping agents and decomposition products were removed by precipitation and re-dispersion cycles with methanol and chloroform, respectively.

NLS/TP peptide coating of QDs. The peptide coating of QDs was done in Igepal reverse micelles (0.11M). To the 4 mL of micelles, 100 μL of NLS and 100 μL of TP (10 mg/mL of water) were added and stirred for ~ 5 min until the solution became clear. To deprotonate the carboxyl and thiol groups, 100 μL of TMAH (tetramethyl ammonium hydroxide in 2-propanol/methanol mixture) was added. Finally, 100 μL of TOPO-capped CdSe/ZnS QDs (5 mg/mL of chloroform) was added and stirred for 18 h. The peptide-coated QDs in the microemulsion were flocculated by the addition of ~ 2 mL of ethanol and centrifuged at 6000 rpm for 5 min. The fluorescent pellet was washed with 1 : 1 volume of cyclohexane and ethanol, and centrifuged one more time. The dried pellet was readily soluble in de-ionized water. The pH of the coated particles in water was ~ 7 .

Bioconjugation of biotinylated peptides with streptavidin-QDs. 50 nM concentration of streptavidin-conjugated QDs were prepared in a 100 μL of PBS containing 5% BSA. The biotinylated MTAS-NLS peptides were added to the streptavidin-conjugated QDs and incubated at room temperature for 15 min. The peptide-coated QDs were diluted further to 200 μL with DMEM. 100 μL of the peptide-coated QDs was added to the cells grown on cover glasses and incubated as described below.

hMSC labeling with QD-peptide conjugates. hMSCs were obtained from Lonza (Singapore) and cultured with the MSCGM (Lonza, Singapore) media. The cells were used for experiments within five passages of culture. Approximately, 50,000 cells were seeded onto cover glasses placed in a 6-well plate. The QD-peptide conjugates were added to the cells in serum-free media. The cells were incubated for 30 min at 37°C . The cells were washed with PBS and fixed with 4% formaldehyde. The cover glasses were mounted on a slide and observed in a fluorescence microscope (Olympus); images acquired were processed using Image J software.

Nocodazole treatment of hMSCs. hMSCs grown on cover glasses were exposed to 5 $\mu\text{g}/\text{ml}$ of nocodazole in the growth media for 4 h prior to QD addition. The



disruption of the cytoskeletal elements was verified with phalloidin staining. The cells were further incubated with QDs for 30 min. The cells were fixed as described earlier and observed under fluorescence microscope.

Confocal laser scanning microscopy imaging and z-stack analysis. The cells were incubated with I-MTAS-QDs (red) as described earlier. Cells were fixed and subjected to immunostaining with anti-alpha-tubulin monoclonal antibody (mouse IgG1 isotype from Sigma, Singapore) and diluted 1:200 in PBS containing 5% BSA. Anti-mouse secondary antibody conjugated with Alexa Fluor-488 dye was used as the secondary antibody to detect tubulin filaments (green); further nuclei were labeled with DAPI (blue). The samples were imaged under confocal microscope (Zeiss LSM 510 META, Biopolis Shared Facility, Singapore). Orthogonal analysis was done on the z-stack images using ImageJ software.

- Gao, X., Cui, Y., Levenson, R. M., Chung, L. W. & Nie, S. In vivo cancer targeting and imaging with semiconductor quantum dots. *Nat. Biotechnol.* **22**, 969–976 (2004).
- Medintz, I. L., Uyeda, H. T., Goldman, E. R. & Mattoussi, H. Quantum dot bioconjugates for imaging, labelling and sensing. *Nat. Mater.* **4**, 435–446 (2005).
- Michalet, X. *et al.* Quantum dots for live cells, in vivo imaging, and diagnostics. *Science* **307**, 538–544 (2005).
- Shen, R. *et al.* Multifunctional conjugates to prepare nucleolar-targeting CdS quantum dots. *J. Am. Chem. Soc.* **132**, 8627–8634 (2010).
- Jiang, W., Kim, B. Y., Rutka, J. T. & Chan, W. C. Nanoparticle-mediated cellular response is size-dependent. *Nat. Nanotechnol.* **3**, 145–150 (2008).
- Kim, B. *et al.* Tuning payload delivery in tumour cylindroids using gold nanoparticles. *Nat. Nanotechnol.* **5**, 465–472 (2010).
- Petros, R. A. & DeSimone, J. M. Strategies in the design of nanoparticles for therapeutic applications. *Nat. Rev. Drug Discov.* **9**, 615–627 (2010).
- Krpetec, Z. *et al.* Negotiation of intracellular membrane barriers by TAT-modified gold nanoparticles. *ACS Nano* **5**, 5195–5201 (2011).
- Wei, Y., Jana, N. R., Tan, S. J. & Ying, J. Y. Surface coating directed cellular delivery of TAT-functionalized quantum dots. *Bioconjugate Chem.* **20**, 1752–1758 (2009).
- Lagerholm, B. C. *et al.* Multicolor coding of cells with cationic peptide coated quantum dots. *Nano Lett.* **4**, 2019–2022 (2004).
- Anas, A. *et al.* Clathrin-mediated endocytosis of quantum dot-peptide conjugates in living cells. *ACS Nano* **3**, 2419–2429 (2009).
- Smith, B. R. *et al.* Real-time intravital imaging of RGD-quantum dot binding to luminal endothelium in mouse tumor neovasculature. *Nano Lett.* **8**, 2599–2606 (2008).
- Ruan, G., Agrawal, A., Marcus, A. I. & Nie, S. Imaging and tracking of Tat peptide-conjugated quantum dots in living cells: new insights into nanoparticle uptake, intracellular transport, and vesicle shedding. *J. Am. Chem. Soc.* **129**, 14759–14766 (2007).
- Delehanty, J. B. *et al.* Self-assembled quantum dot-peptide bioconjugates for selective intracellular delivery. *Bioconjugate Chem.* **17**, 920–927 (2006).
- Chen, F. & Gerion, D. Fluorescent CdSe/ZnS nanocrystal-peptide conjugates for long-term, nontoxic imaging and nuclear targeting in living cells. *Nano Lett.* **4**, 1827–1832 (2004).
- Folkman, J. Angiogenesis: an organizing principle for drug discovery? *Nat. Rev. Drug Discov.* **6**, 273–286 (2007).
- Pooga, M. *et al.* Cellular translocation of proteins by transportan. *The FASEB Journal* **15**, 1451–1453 (2001).
- Muratovska, A. & Eccles, M. R. Conjugate for efficient delivery of short interfering RNA (siRNA) into mammalian cells. *FEBS Lett.* **558**, 63–68 (2004).
- Koppelhus, U. & Nielsen, P. E. Cellular delivery of peptide nucleic acid (PNA). *Adv. Drug Deliv. Rev.* **55**, 267–280 (2003).
- Chan, W. C. & Nie, S. Quantum dot bioconjugates for ultrasensitive nonisotopic detection. *Science* **281**, 2016–2018 (1998).
- Mattoussi, H. *et al.* Self-assembly of CdSe-ZnS quantum dot bioconjugates using an engineered recombinant protein. *J. Am. Chem. Soc.* **122**, 12142–12150 (2000).
- Pathak, S., Choi, S. K., Arnheim, N. & Thompson, M. E. Hydroxylated quantum dots as luminescent probes for in situ hybridization. *J. Am. Chem. Soc.* **123**, 4103–4104 (2001).
- Pinaud, F., King, D., Moore, H. P. & Weiss, S. Bioactivation and cell targeting of semiconductor CdSe/ZnS nanocrystals with phytochelatin-related peptides. *J. Am. Chem. Soc.* **126**, 6115–6123 (2004).
- Yi, D. K. *et al.* Silica-coated nanocomposites of magnetic nanoparticles and quantum dots. *J. Am. Chem. Soc.* **127**, 4990–4991 (2005).
- Tan, T. T., Selvan, S. T., Zhao, L., Gao, S. & Ying, J. Y. Size control, shape evolution, and silica coating of near-infrared-emitting PbSe quantum dots. *Chem. Mater.* **19**, 3112–3117 (2007).

- Selvan, S. T., Tan, T. T. & Ying, J. Y. Robust, Non-cytotoxic, silica-coated CdSe quantum dots with efficient photoluminescence. *Adv. Mater.* **17**, 1620–1625 (2005).
- Selvan, S. T., Patra, P. K., Ang, C. Y. & Ying, J. Y. Synthesis of silica-coated semiconductor and magnetic quantum dots and their use in the imaging of live cells. *Angew. Chem. Int. Ed.* **46**, 2448–2452 (2007).
- Zhang, F. *et al.* Polymer-Coated Nanoparticles: A universal tool for biolabelling experiments. *Small* **7**, 3113–3127 (2011).
- Duan, H. & Nie, S. Cell-penetrating quantum dots based on multivalent and endosome-disrupting surface coatings. *J. Am. Chem. Soc.* **129**, 3333–3338 (2007).
- Schieber, C. *et al.* Conjugation of transferrin to azide-modified CdSe/ZnS core-shell quantum dots using cyclooctyne click chemistry. *Angew. Chem. Int. Ed.* **51**, 10523–10527 (2012).
- Vale, R. D. The molecular motor toolbox for intracellular transport. *Cell* **112**, 467–480 (2003).
- Arnold, D. B. Actin and microtubule-based cytoskeletal cues direct polarized targeting of proteins in neurons. *Sci. Signal* **2**, pe49 (2009).
- Roth, D. M., Moseley, G. W., Glover, D., Pouton, C. W. & Jans, D. A. A microtubule-facilitated nuclear import pathway for cancer regulatory proteins. *Traffic* **8**, 673–686 (2007).
- Giannakakou, P. *et al.* p53 is associated with cellular microtubules and is transported to the nucleus by dynein. *Nat. Cell Biol.* **2**, 709–717 (2000).
- Lam, M. H. *et al.* Nuclear transport of parathyroid hormone (PTH)-related protein is dependent on microtubules. *Mol. Endocrinol.* **16**, 390–401 (2002).
- Roth, D. M., Moseley, G. W., Pouton, C. W. & Jans, D. A. Mechanism of microtubule-facilitated "fast track" nuclear import. *J. Biol. Chem.* **286**, 14335–14351 (2011).
- Rajendran, L., Knölker, H.-J. & Simons, K. Subcellular targeting strategies for drug design and delivery. *Nat. Rev.* **9**, 29–42 (2010).
- Liu, X., Yu, M., Kim, H., Mameli, M. & Stellacci, F. Determination of monolayer-protected gold nanoparticle ligand-shell morphology using NMR. *Nat. Commun.* **3**, 1182, doi: 10.1038/ncomms2155 (2012).
- Verma, A. *et al.* Surface Structure-Regulated Cell Membrane Penetration by Monolayer Protected Nanoparticles. *Nat. Mater.* **7**, 588–595 (2008).
- Xu, J. *et al.* Nanoblade delivery and incorporation of quantum dot conjugates into tubulin networks in live cells. *Nano Lett.* **12**, 5669–5672 (2012).
- Peng, Z. A. & Peng, X. Formation of high-quality CdTe, CdSe, and CdS nanocrystals using CdO as precursor. *J. Am. Chem. Soc.* **123**, 183–184 (2001).
- Peng, Z. A. & Peng, X. Nearly monodisperse and shape-controlled CdSe nanocrystals via alternative routes: nucleation and growth. *J. Am. Chem. Soc.* **124**, 3343–3353 (2002).

Acknowledgements

This work was supported by IMRE, A*STAR (Agency for Science, Technology and Research, Singapore) Joint Council Office (JCO) Grant: JCOAG03_FG03_2009, and IBN (Biomedical Research Council, A*STAR).

Author contributions

K.N. designed the experiments and contributed to the experimental analysis and interpretation of data, and wrote the manuscript. S.K. contributed to the experiments and analysis. Q.D. contributed to the experiments and analysis. P.P. contributed to the experiments and analysis. T.S. contributed to the interpretation of the experimental data and contributed to the writing of the manuscript. S.A. contributed to the interpretation of the experimental data and contributed to the writing of the manuscript. J.Y.Y. contributed to the interpretation of the experimental data and contributed to the editing of the manuscript. S.T.S. conceived the work and designed the experiments, contributed to the interpretation of the experimental data and wrote the manuscript with revisions from other coauthors.

Additional information

Supplementary information accompanies this paper at <http://www.nature.com/scientificreports>

Competing financial interests: The authors declare no competing financial interests.

How to cite this article: Narayanan, K. *et al.* Mimicking cellular transport mechanism in stem cells through endosomal escape of new peptide-coated quantum dots. *Sci. Rep.* **3**, 2184; DOI:10.1038/srep02184 (2013).



This work is licensed under a Creative Commons Attribution-NonCommercial-NoDerivs 3.0 Unported license. To view a copy of this license, visit <http://creativecommons.org/licenses/by-nc-nd/3.0>